Relationship Between Foveal Cone Structure and Clinical Measures of Visual Function in Patients With Inherited Retinal Degenerations

Kavitha Ratnam,[1,2] Joseph Carroll,[3–5] Travis C. Porco,[1,6,7] Jacque L. Duncan,[1] and Austin Roorda[2]

[1]Department of Ophthalmology, University of California, San Francisco, San Francisco, California
[2]School of Optometry, University of California, Berkeley, Berkeley, California
[3]Department of Ophthalmology, Medical College of Wisconsin, Milwaukee, Wisconsin
[4]Department of Biophysics, Medical College of Wisconsin, Milwaukee, Wisconsin
[5]Department of Cell Biology, Neurobiology and Anatomy, Medical College of Wisconsin, Milwaukee, Wisconsin
[6]The Francis I. Proctor Foundation for Research in Ophthalmology, University of California, San Francisco, San Francisco, California
[7]Division of Preventive Medicine and Public Health, Department of Epidemiology and Biostatistics, University of California, San Francisco, San Francisco, California

Correspondence: Austin Roorda, School of Optometry, University of California, Berkeley, 485 Minor Hall, Berkeley, CA 94720-2020; aroorda@berkeley.edu.

Submitted: June 6, 2013
Accepted: July 25, 2013

Citation: Ratnam K, Carroll J, Porco TC, Duncan JL, Roorda A. Relationship between foveal cone structure and clinical measures of visual function in patients with inherited retinal degenerations. *Invest Ophthalmol Vis Sci.* 2013;54:5836–5847. DOI:10.1167/iovs.13-12557

Purpose. To study the relationship between cone spacing and density and clinical measures of visual function near the fovea.

Methods. High-resolution images of the photoreceptor mosaic were obtained with adaptive optics scanning laser ophthalmoscopy from 26 patients with inherited retinal degenerations. Cone spacing measures were made close to or at the foveal center (mean [SD] eccentricity, 0.02 [0.03] degree; maximum eccentricity, 0.13 degree) and were converted to *Z*-scores, fraction of cones, and percentage-of-cones-below-average compared with normal values for each location (based on 37 age-similar visually normal eyes). *Z*-scores and percentage of cones below average were compared with best-corrected visual acuity (VA) and foveal sensitivity.

Results. Visual acuity was significantly correlated with cone spacing (Spearman rank correlation $\rho = -0.60$, $P = 0.003$) and was preserved ($\geq$80 letters), despite cone density measures that were 52% below normal. Foveal sensitivity showed significant correlation with cone spacing ($\rho = -0.47$, $P = 0.017$) and remained normal ($\geq$35 decibels), despite density measures that were approximately 52% to 62% below normal.

Conclusions. Cone density was reduced by up to 62% below normal at or near the fovea in eyes with VA and sensitivity that remained within normal limits. Despite a significant correlation with foveal cone spacing, VA and sensitivity are insensitive indicators of the integrity of the foveal cone mosaic. Direct, objective measures of cone structure may be more sensitive indicators of disease severity than VA or foveal sensitivity in eyes with inherited retinal degenerations. (ClinicalTrials.gov number, NCT00254605.)

Keywords: adaptive optics, cone structure, fovea, visual acuity, cone sensitivity

Because of its importance in fine visual resolution and its long-term preservation in rod-cone degenerations, foveal vision is commonly used to monitor visual health and track disease progression. However, the most common foveal functional measure, visual acuity (VA), is preserved until late in the course of rod-cone degeneration compared with other measures. Patients with good Snellen VA (20/30 or better) have shown significant foveal cone abnormalities assessed via contrast sensitivity,[1–3] foveal thresholds,[4] and foveal cone dysfunction measured by focal electroretinography.[5] In addition, intrasubject variability in psychophysical techniques such as VA[6–9] and sensitivity[10–12] makes it difficult to objectively quantify the extent of foveal degeneration. Increased disease severity has been correlated with increased variability in these test results,[8,13,14] and ophthalmologists generally consider a minimum change of 2 lines (10 letters) on the Snellen acuity chart to be clinically significant.[15] The slow progression and variability of functional measures of photoreceptor survival make the assessment of disease progression and treatment response unreliable and challenging. Previous studies[16–19] of inherited retinal degenerations have demonstrated that slowly changing and unreliable conventional functional measures display anywhere from 5-year to 15-year half-life times of visual field loss.

As such, efforts have been made to explore the use of objective measures of cone structure as a more robust and sensitive indicator of foveal degeneration. However, disparities exist between psychophysical and anatomical data. Studies have shown that functional foveal performance remains at relatively high levels, despite large structural changes. For example, cone photopigment optical density reductions occur in retinitis pigmentosa (RP), despite normal acuity.[20–22] Geller and Sieving[23] reported that patchy loss of 90% of foveal cones was necessary to give rise to significant reductions in grating acuity, although this number was obtained from modeling estimates, rather than direct visualization of cone topography.

To determine the mechanism of acuity loss in patients with RP, Alexander et al.[24] used grating, Vernier, and letter acuities and concluded that increased foveal cone spacing, rather than reduced cone photopigment optical density, was responsible for lowered acuity. In a separate histologic study,[25] abnormal foveal cone spacing was observed in a patient having RP with normal acuity.

Previously, structural assessment of the living retina was precluded by the low optical and sampling resolution of conventional imaging systems. In the past few decades, however, the development of optical coherence tomography (OCT) and adaptive optics (AO) as high-resolution, noninvasive instruments for retinal imaging has potentiated a major advance in clinical ophthalmology. Optical coherence tomography is a low-coherence interferometric technique with an axial resolution of 1 to 15 μm[26,27] that has been used to relate visual function with structural measures of foveal degeneration, including inner segment/outer segment (IS/OS) junction integrity and foveal thickness. The presence of a distinct, continuous IS/OS junction in OCT images generally indicates the normal alignment and functioning of photoreceptor OS discs,[28] and IS/OS disruption has been shown to correlate with reduced VA in patients with inherited retinal degenerations.[28–30] Similarly, foveal thinning attributed to cone death has been associated with significant VA loss[29,31,32] and elevated foveal thresholds[33] in the diseased retina. Although these studies have assessed OCT structure-function correlations over broad ranges of disease severity (range, 20/15–20/1000 VA[29]), none to date have reported on the relationship for a narrower range of VAs. However, OCT abnormalities have been observed in patients with good acuity and foveal thresholds,[28,34–36] suggesting that structural measures may provide a more sensitive measure of disease than visual function.

Adaptive optics is a set of techniques that are used to compensate for aberrations in living eyes and has been used to improve retinal images to a lateral resolution of approximately 2 μm,[37–40] enabling direct visualization of the cone mosaic and measurement of cone spacing and density in normal and diseased eyes.[34,35,41–52] Adaptive optics–based studies[41,42] of retinal degeneration showed a significant correlation between macular cone spacing and central visual function, but given the small size and unique anatomy[53] of foveal cones and the resulting difficulties posed on imaging,[54] these studies were unable to assess cone morphology at the foveal center. Within the past few years, advanced systems that have implemented improvements in AO scanning laser ophthalmoscopy (AOSLO) system design[55] and advanced controls[56] have been able to more routinely visualize the foveal cone mosaic.[57] To date, AOSLO foveal cone measures have been used to characterize changes in myopia[58] and relationships between resolution and neural sampling[59] in healthy eyes. There is a growing body of studies[35,47,60] on cone spacing in the foveal center, but comparisons between in vivo foveal cone structure and standard measures of visual function in a larger cohort of patients with retinal degeneration have yet to be evaluated.

In the present study, we describe foveal cone spacing and density in eyes with retinal degenerations from high-resolution, in vivo images of the fovea acquired with AOSLO and compare these measures with best-corrected VA (BCVA) and foveal sensitivity in the same eyes in 26 patients. To assess whether cone structure is a more sensitive indicator of disease severity than clinical measures of visual function, cone density values below normal were used to assess changes in foveal morphology in patients with retinal degenerations who had a range of BCVA and foveal sensitivity values.

Methods

Study Design

Research procedures followed the tenets of the Declaration of Helsinki, and informed consent was obtained from all subjects. The study protocol was approved by the institutional review boards of the University of California, San Francisco; the University of California, Berkeley; and the Medical College of Wisconsin.

Subjects

Twenty-six patients (18 female and 8 male) with inherited retinal degenerations from 23 unrelated families were characterized clinically (Table 1). Patients were excluded if they had other ocular or systemic conditions that could affect VA, including cataract, amblyopia, and cystoid macular edema involving the fovea. Subjects characterized in earlier studies are included in Table 1.

Clinical Examination

Best-corrected VA was measured using a standard eye chart according to the Early Treatment of Diabetic Retinopathy Study (ETDRS) protocol.[61] Automated perimetry was completed using a 10-2 Swedish interactive threshold algorithm (SITA) with measurement of foveal thresholds using a Goldmann III stimulus on a white background (10.03 cd/m^2) and exposure duration of 200 ms (Humphrey Visual Field Analyzer HFA II 750-6116-12.6; Carl Zeiss Meditec, Inc., Dublin, CA). Foveal sensitivity was expressed in the logarithmic decibel scale (dB = 10 × log [1/Lambert]) and in the linear scale (1/Lambert).

AOSLO Image Acquisition and Cone Spacing and Density Analysis

Pupils were dilated with 1% tropicamide and 2.5% phenylephrine before AOSLO imaging. High-resolution images were obtained using AOSLO for the 26 patients and 37 age-similar visually normal subjects, and images were processed to create montages of the macular region. For the patients measured at the University of California, Berkeley ($n = 22$), the region of the fovea used for fixation (preferred retinal locus [PRL]) was determined by recording a 10-second to 15-second video as the patient looked at a target delivered through modulation of the AOSLO scanning raster.[62] The fixation target was encoded directly into the video, and the mean (SD) locations of fixation points in the horizontal (SD_x) and vertical (SD_y) directions relative to the retina were determined using custom image analysis tools written in MATLAB (The MathWorks, Inc., Natick, MA). For the patients measured at the Medical College of Wisconsin ($n = 4$), the embedded fixation target was not available, so we assumed that the patients used the location of maximum cone density as their PRL. The PRL and the position of maximum cone density are similar but have been shown to differ on average by 6 to 10 minutes of arc (arc min).[58,63] The eye in which unambiguous cone mosaics could be visualized closest to the PRL was selected for cone spacing measurements. Customized software was used to determine quantitative cone spacing measures using previously described methods,[41] and cone spacing measurements for the patients were compared with those of the 37 visually normal subjects. For the control data set, the foveal center (eccentricity, 0 degree) was defined as the location of peak foveal cone density when known ($n = 11$); for the remaining 26 subjects, the foveal center was identified as the PRL. Cone locations in patients

Table 1. Summary of Clinical and Structural Characteristics of Patients Studied

					VA		Humphrey 10-2 Foveal Sensitivity		PRL		Foveal Cone Spacing		
Patient No.	Age, y/ Sex	Eye	Condition	Source (Subject ID)	BCVA	ETDRS, Letters	Logarithmic, dB	Linear, 1/Lambert	Location	SD_x, SD_y Fixational Stability, Arc Min	Z-Score	Average Eccentricity From PRL, Arc Min (Deg)	Cones Below Average, %
1	17/M	Left	CHM	Syed et al.,[95] 2013 (D-IV-3)	20/25	80	34*	2511.89*	Fixation target	4.51, 3.86	2.07	1.62 (0.03)	38.02
2	38/F	Right	CHM carrier	Syed et al.,[95] 2013 (D-III-2)	20/16	88	36	3981.07	Fixation target	3.32, 3.14	2.38	1.07 (0.02)	41.64
3	26/F	Left	CHM carrier	Syed et al.,[95] 2013 (A-V-2)	20/20	85	38	6309.57	Fixation target	2.17, 5.52	2.97	1.8 (0.03)	48.14
4	27/F	Left	CHM carrier	Syed et al.,[95] 2013 (B-V-3)	20/20	85	36	3981.07	Fixation target	3.56, 8.92	2.72	0.82 (0.01)	45.33
5	37/F	Right	ADRP	Talcott et al.,[51] (1)	20/16	89	37	5011.87	Fixation target	1.95, 2.95	0.28	0.36 (0.01)	6.87
6	45/F	Right	ADRP	...	20/25	83	35	3162.28	Peak cone density	NA	−0.97	0.00	−30.40
7	38/F	Right	Simplex RP	...	20/32	81	34*	2511.89*	Fixation target	4.71, 2.54	5.88	8.08 (0.13)	69.90
8	48/F	Left	Simplex RP	...	20/25	80	34*	2511.89*	Fixation target	1.09, 0.89	3.07	7.57 (0.13)	50.85
9	40/M	Right	Simplex RP	...	20/20	83	37	5011.87	Fixation target	4.20, 1.66	−0.20	0.40 (0.01)	−5.34
10	28/F	Left	Simplex RP	...	20/25	82	39	7943.28	Fixation target	3.66, 6.24	2.61	1.62 (0.03)	44.37
11	32/F	Right	Simplex RP	...	20/40	62*	12*	15.85*	Fixation target	1.61, 2.37	5.44	0.90 (0.01)	65.64
12	40/F	Right	Simplex RP	...	20/16	89	37	5011.87	Fixation target	3.76, 8.55	0.29	0.36 (0.01)	7.04
13	30/M	Right	Multiplex RP	...	20/25	81	34*	2511.89*	Fixation target	4.43, 2.67	3.06	2.49 (0.04)	49.17
14	30/M	Right	XLRP	...	20/50	63*	25*	316.23*	Fixation target	1.65, 3.50	2.37	0.76 (0.01)	41.41
15	49/F	Left	XLRP carrier	...	20/12.5	93	35	3162.28	Fixation target	6.23, 3.30	−0.32	0.85 (0.01)	−8.98
16	20/F	Left	XLRP carrier	...	20/50	67*	32*	1584.89*	Fixation target	5.49, 2.98	7.08	1.44 (0.02)	72.95
17	18/F	Right	NARP	Yoon et al.,[35] 2009 (II-4)	20/50	65*	32*	1584.89*	Fixation target	9.90, 4.08	5.01	0.69 (0.01)	63.19
18	22/F	Left	NARP	Yoon et al.,[35] 2009 (II-3)	20/25	79*	35	3162.28	Fixation target	1.72, 2.65	3.90	0.51 (0.01)	55.82
19	50/F	Left	NARP	Yoon et al.,[35] 2009 (I-1)	20/50	65*	27*	501.19*	Fixation target	8.67, 3.07	7.61	0.70 (0.01)	74.61
20	27/F	Left	NARP	Yoon et al.,[35] 2009 (II-2)	20/16	90	38	6309.57	Fixation target	3.84, 3.63	2.55	0.40 (0.01)	43.36
21	26/M	Left	USH2	...	20/25	77*	33*	1995.26*	Peak cone density	NA	2.29	0.00	40.30
22	34/M	Right	USH2	Talcott et al.,[51] (2)	20/20	85	36	3981.07	Fixation target	1.53, 1.62	2.15	0.75 (0.01)	38.86
23	33/M	Right	USH2	...	20/20	85	39	7943.28	Peak cone density	NA	−0.41	0.00	−11.47
24	29/F	Left	USH2	...	20/30	80	32*	1584.89*	Peak cone density	NA	2.33	0.00	40.83
25	20/M	Left	USH3	Ratnam et al.,[34] 2013 (1)	20/16	90	36	3981.07	Fixation target	3.60, 2.40	1.86	0.62 (0.01)	35.04
26	25/F	Right	USH3	Ratnam et al.,[34] 2013 (2)	20/20	85	35	3162.28*	Fixation target	2.77, 3.33	−0.86	0.00 (0.05)	−26.47

For patients characterized using AOSLO in previous studies, references and subject IDs are included in the table. ADRP, autosomal dominant RP; CHM, choroideremia; NA, not available; NARP, neurogenic weakness, ataxia, RP; USH2, Usher syndrome type 2; USH3, Usher syndrome type 3; XLRP, X-linked RP.

* Abnormal values for ETDRS score and foveal sensitivity.

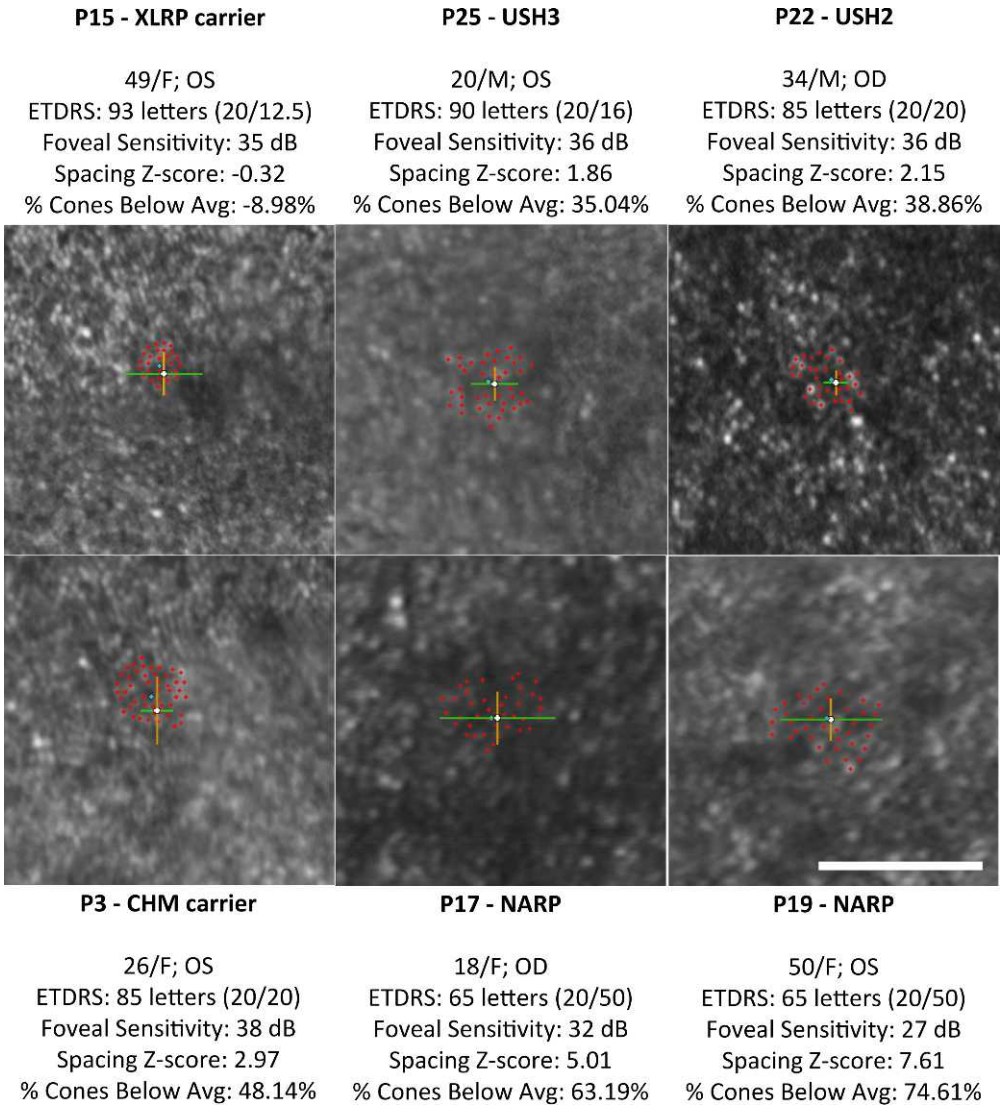

Figure 1. Adaptive optics scanning laser ophthalmoscopy images ($0.5° \times 0.5°$) of foveal cone mosaics in six subjects' eyes, centered around the PRL of fixation (*white crossbairs*). Patients are arranged by increasing percentage of cones below average from *left* to *right* and *top* to *bottom*. *Red crossbairs* indicate cone selections used to calculate cone spacing *Z*-scores and percentage of cones below average, with *blue diamonds* indicating the average location of cone selections. *Green lines* and *orange lines* indicate 1 SD of fixation from the average PRL location in the *horizontal* and *vertical* directions, respectively. *White scale bar*: 0.25°.

were measured as eccentricity in degrees relative to the PRL or location of peak cone density, and cone spacing in patients was measured close to or at the PRL (mean [SD] eccentricity, 0.02 [0.03] degree; maximum eccentricity, 0.13 degree). *Z*-scores were computed as the number of SDs from the normal mean cone spacing at the eccentricity measured; *Z*-scores between −2 and 2 (±SD) were considered normal.

Assuming regular, hexagonal packing of cones, cone spacing at tested locations was converted into cone density using a previously published method.[35] As such, cone density as reported must be considered an upper estimate of the density of the cone mosaic in these individuals at these locations. We adopted this approach to compute density for two reasons. First, not all cones are visible at the fovea, even with AO, so densities based on subjective identification of every visible cone will likely be underestimated (see Fig. 1 for examples). Second, fine spatial tasks are likely mediated by small patches of contiguous cones,[64] and our method to estimate cone density within these patches is adequate. Cone density (*D*) was converted into fraction of cones (FOC) compared with average using the following equation: $\text{FOC} = D_{\text{subject}}/D_{\text{normal, average}}$. This was used to compute percentage of cones below average (i.e., the difference in the patient's cone density at a given eccentricity from the average value for the 37 visually normal subjects) using the following equation: $\%\ \text{Cones Below Average} = 100\ (1 - \text{FOC})$.

Negative values for percentage of cones below average indicate that cone density was greater than average at that location. Cone spacing *Z*-scores within 2 SD at the foveal center correspond to cone densities up to 36.7% below (*Z*-score = 2) or above (*Z*-score = −2) the normal mean at the foveal center, which may be attributable to the high individual variability of human foveal cone density.[53,58,65–68] Therefore, percentage of cones below average does not necessarily indicate percentage of cone loss; however, when the *Z*-scores exceed 2, there is a strong likelihood that foveal cone loss has occurred.

Statistical Analysis

Z-scores were compared with ETDRS scores and foveal sensitivity using Spearman rank correlation ρ, which computes the correlation between the ranked order of variables and is unaffected by the nonlinearity of monotonic relationships between variables. *P* values were calculated using the Holm adjustment; $P < 0.05$ was considered statistically significant.

Percentage of cones below average was plotted against VA and foveal sensitivity. The threshold for cone percentage beyond which the ETDRS score dropped below 85 letters (~20/20) and 80 letters (~20/25)[69] was determined. Similarly, the threshold for cone percentage beyond which foveal sensitivity dropped below normal values (<35 dB in the logarithmic scale; <3162.28 1/Lambert in the linear scale) was determined. The data were fit to a locally weighted scatter plot smoothing curve, and 95% confidence intervals (CIs) were obtained using the cases bootstrap method.[70]

Results

Clinical characteristics of the patients are summarized in Table 1. The patients (18 female and 8 male) ranged in age from 17 to 50 years (mean [SD] age, 31.9 [9.6] years), and the visually normal subjects (20 female and 17 male) were similar in age (age range, 14–58 years; mean [SD] age, 31.3 [12.2] years). Patients' ETDRS acuity ranged from 93 to 62 letters (mean [SD] acuity, 80.5 [8.9] letters), and foveal sensitivities ranged from 39 to 12 dB (mean [SD] sensitivity, 33.8 [5.5] dB). Normal ETDRS acuity ranged from 93 to 80 letters, and normal foveal sensitivity ranged from 39 to 35 dB. Patients retained mean (maximum) stable foveal fixation of 3.84 (9.90) arc min for SD*x* and 3.63 (8.92) arc min for SD*y*, which is similar to the range observed in visually normal subjects (1–5 arc min[63,71–73]). The average location of cone selections for each patient was within 1 SD of the PRL, except for patient 7 and patient 8, whose image quality precluded cone selections at the PRL. Cone spacing *Z*-scores ranged from –0.97 (30.4% cones above the normal average number of cones) to 7.61 (74.6% cones below the normal average number of cones). Figure 1 shows examples of foveal cone mosaics with varying *Z*-scores.

Visual acuity (Fig. 2) and foveal sensitivity in logarithmic and linear units (Fig. 3) are plotted against *Z*-scores and percentage of cones below average. Table 2 summarizes the statistical analyses. A statistically significant correlation was found between cone spacing *Z*-scores and ETDRS acuity ($\rho = -0.60$, $P = 0.003$) and between *Z*-scores and foveal sensitivity in logarithmic and linear units ($\rho = -0.47$, $P = 0.017$ for both scales). When plotted against percentage of cones below average, the cone percentage decreases before abnormal acuity was observed were 24.82% (95% CI, 1.77%–43.59%) for fewer than 85 letters (20/20 acuity) and 51.75% (95% CI, 34.16%–65.83%) for fewer than 80 letters (20/25 acuity) (Fig. 2). Cone percentages below average for abnormal logarithmic and linear foveal sensitivities were 51.66% (95% CI, 17.90%–67.27%) and 61.85% (95% CI, 46.58%–69.90%), respectively (Fig. 3).

Discussion

This study presents the first cross-sectional assessment to date of in vivo foveal cone structure and conventional measures of visual function in patients with inherited retinal degenerations. Although previous studies[34,35,41–52] have used AOSLO to assess cone spacing and density in normal and diseased eyes, none have reported on how foveal cone measures and visual function are correlated. The present study demonstrates a significant correlation between increased AOSLO cone spacing *Z*-scores and decreased VA at or near the fovea, as well as a significant correlation between *Z*-scores and foveal sensitivity. When converted to cone density, preserved VA (>20/40) and normal foveal sensitivity in decibel and linear units were observed even when cone density was 52% to 62% below the normal average.

Normal Variability of Human Foveal Cone Density

Because of high individual variability in foveal cone density,[53,58,65–68] comparisons of foveal cone spacing and density between patients and normative data cannot be used to directly estimate photoreceptor loss. In the present study, cone spacing *Z*-scores within 2 SD were considered normal; when converted to density, a spacing *Z*-score of 2 corresponded to a cone percentage decrease of approximately 36.7% from the normal mean.

Histologic evidence indicates that, although peak cone density in humans is highly variable, the total number of cones near the foveal center is relatively constant.[66] However, Song et al.[68] observed up to a 25% decrease in cone packing density in older (age range, 50–65 years) versus younger (age range, 22–35 years) subjects within 0.5 mm of the foveal center, which is inclusive of the PRL, and age-dependent changes in foveal cone density have been reported elsewhere.[74] Although our patients had an age distribution (age range, 17–50 years; mean [SD] age, 31.9 [9.6] years) similar to that of our normative database (age range, 14–58 years; mean [SD] age, 31.3 [12.2] years), comparison of patient and normative data within smaller age ranges (e.g., by decade) might have further reduced variability effects. The limited size of our normal data set prevented more stringent age-matched comparisons. Despite these limitations, our calculated threshold for cone densities below which measurable losses of function occur was lower than the lower bound of cone densities attributable to normal variability (~36.7% cones below average), except for ETDRS acuity less than 85 letters (threshold of 24.8% cones below average) (Table 2). Therefore, although our results do not provide exact measurements of cone loss, they suggest that VA (>20/40) and foveal sensitivity are preserved even when cone density is substantially lower than normal near or at the foveal center.

Comparison of AOSLO Normative Cone Measures With Histologic Data

To assess whether the normative data used in this study are in agreement with histologic measurements, AOSLO cone spacing measures at the foveal center were converted into density and compared with histologic data by Curcio et al.[66] among seven subjects (mean [SD] histologic peak foveal cone density, 199,200 [87,200] cones/mm^2; range, 98,200–324,100 cones/mm^2). To convert angular cone density (in cones per degree squared) to retinal distances (in cones per millimeter squared), the assumption of 289 μm/deg was used,[47,75,76] producing a mean AOSLO foveal density of 127,774.27 cones/mm^2 (95% CI, 85,297.41–235,152.41 cones/mm^2), which is within 1 SD of the data by Curcio et al., although reduced by 35.9%. This reduction may be because of the larger sample size of the AOSLO normative data set ($n = 37$), which may be less susceptible to the effects of variability and provide a more generalized mean foveal cone density value than that of the smaller histologic data set ($n = 7$). In addition, the PRL was assumed to correspond to the anatomical foveal center for 26 of the 37 normal AOSLO eyes (for whom the location of peak cone density was unknown), so the mean density value was likely lower than it would have been had the peak cone

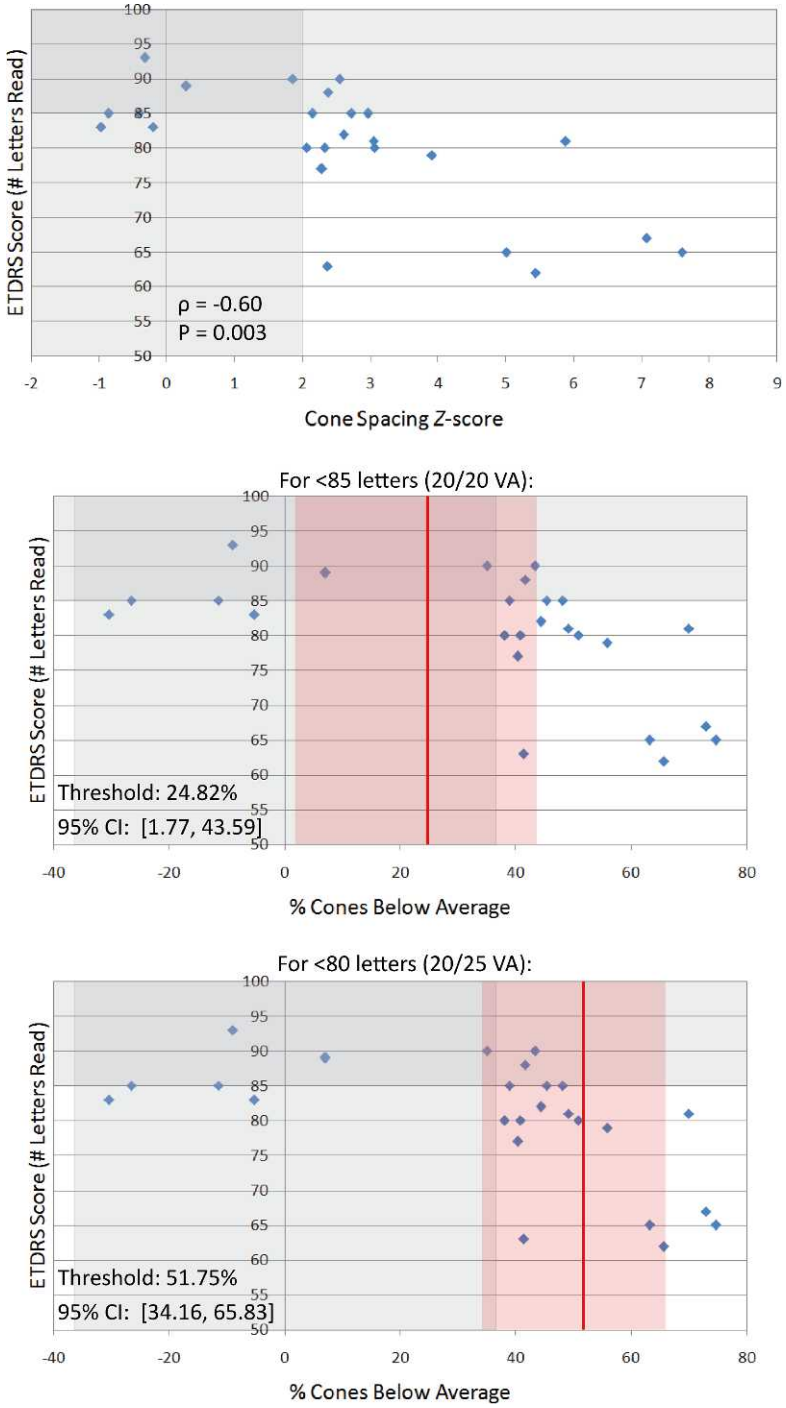

Figure 2. *Top*: Visual acuity measured as ETDRS letter scores correlates with cone spacing *Z*-scores. *Vertically shaded grey region* indicates the range of normal *Z*-scores (±2 SD); *horizontally shaded region* indicates the normal range of VA (100–85 letters). *Center*: Visual acuity plotted against percentage of cones below average. *Vertically shaded grey region* indicates percentage cone values corresponding to the normal range of *Z*-scores; *horizontally shaded grey region* indicates the normal range of VA. *Red line* indicates cone percentage after which ETDRS scores fall below 85 letters (20/20 acuity), which was determined by fitting the data to a locally weighted scatter plot smoothing (LOWESS) curve; *red shaded region* indicates 95% CIs. *Bottom*: Percentage of cones below average with threshold value and 95% CI for EDTRS scores below 80 letters (20/25 acuity).

densities been quantified for all subjects, as was done with the histologic data. However, because cone spacing measurements for the present study were made at or near the PRL, contrast with a normative database mainly based on PRL provides a more similar data set for comparison than if patients' PRL data had been compared with the mean peak cone density in visually normal subjects.

Uncertainty of the Relationship Between PRL and the Location of Peak Cone Density

In four patients for whom the PRL was unknown, the location of peak cone density was used for analysis. Although the PRL is generally displaced from the location of maximum cone density,[58,63] the eye's optical blur reduces VA below the

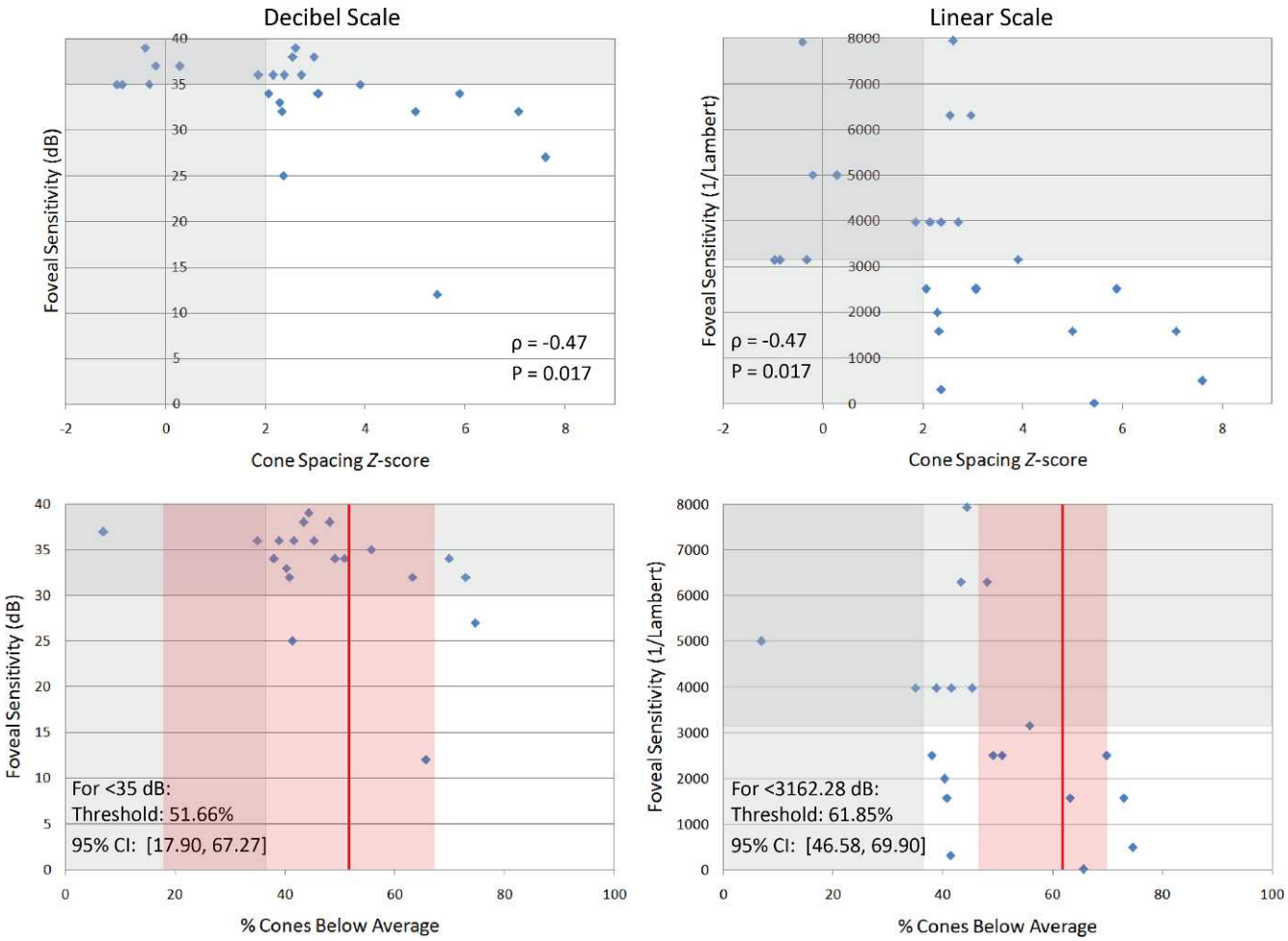

Figure 3. *Top*: Foveal sensitivity in logarithmic (decibel, *left column*) and linear (1/Lambert, *right column*) scales correlates with cone spacing *Z*-scores. *Vertical grey regions* indicate the normal range of *Z*-scores (±2 SD), and *horizontal grey regions* indicate the normal range of sensitivity. *Bottom*: Foveal sensitivity is plotted against percentage of cones below average. *Red vertical lines* indicate cone percentage after which foveal sensitivity became abnormal (<35 dB or <3162.28 1/Lambert), which was determined by fitting the data to a locally weighted scatter plot smoothing (LOWESS) curve; *red shaded regions* indicate 95% CIs.

Nyquist sampling frequency of foveal cones,[77] lessening the effect of absolute cone density on visual function. Weymouth et al.[78] mapped grating acuity in 11-arc min intervals throughout the fovea and did not find that maximum acuity was better anywhere outside of the PRL, suggesting that visual functions at the location of peak cone density and fixation are similar, if not equivalent, and that humans have an excess of foveal cones for high-contrast, photopic acuity tasks. Therefore, the substitution in the present study of peak cone density for comparison with fixational acuity and sensitivity is appropriate, although it may underestimate the extent of cone density reduction occurring at the PRL. The four patients had peak cone densities of 40.83% below to 30.40% above the mean foveal density of visually normal subjects, which was derived mainly from measurements near the PRL; because the patients' PRL cone density is expected to be reduced from maximum cone density, these values likely reflect a lower bound of the cone changes actually occurring at fixation.

Table 2. Summary of Statistical Analyses Showing Correlation Between Cone Spacing and Visual Function

Variable	Spearman Rank Correlation ρ	*P* Value	Cones Below Average, % (95% CI)
VA ETDRS score			
For <85 letters, 20/20 VA	−0.60	0.003	24.82 (1.77–43.59)
For <80 letters, 20/25 VA			51.75 (34.16–65.83)
Foveal sensitivity			
Logarithmic	−0.47	0.017	51.66 (17.90–67.27)
Linear	−0.47	0.017	61.85 (46.58–69.90)

Foveal sensitivities are in logarithmic (decibel) and linear (1/Lambert) scales. $P < 0.05$ is statistically significant. The Cones Below Average column demonstrates that upper limits of cone density change before abnormal values were observed for ETDRS acuity (<85 letters and <80 letters) and foveal sensitivity (<35 dB and <3162.28 1/Lambert).

AOSLO Density Measurements Represent an Upper Bound of Structural Changes

In this study, cone spacing was used to quantify foveal cone structure. Cone spacing represents a conservative measure of cone mosaic integrity[41] and was chosen because reliable spacing estimates can be made even if not all the cones have been identified in an image. Because the conversion from spacing to density assumes a close-packed mosaic, the cone density measures reported herein represent an upper limit of percentage of cone density differences from normal. In other words, actual cone densities are likely to be lower than we report. Nevertheless, the cone density thresholds observed in this study are in agreement with earlier studies in which substantial photoreceptor loss was predicted to be necessary to cause a measurable reduction in visual function. By fitting equations to psychometric functions for patients with Stargardt disease, Geller and Sieving[23] estimated a patchy loss of approximately 90% of cones before significant changes in acuity occurred in these subjects, and in a histopathological study of a patient with juvenile macular degeneration, Eagle et al.[79] reported that the patient maintained 20/30 acuity before his death, despite deterioration of most foveal cones. Similar to the models of degeneration by Geller and Sieving,[23] Seiple et al.[80] used pixel blanking in letter optotypes to simulate foveal cone dropout in patients with RP and determined that a loss of 80% of foveal cones was necessary to reduce acuity below 20/40. Although this study looked at acuity changes attributed solely to a reduction in spatial sampling, ignoring other sensory and perceptual factors, their results support our observations that VA is resilient to significant changes in foveal cone topography.

Longitudinal Studies Would Facilitate Accurate Assessments of Degeneration in Individual Subjects

A limitation of this study was its cross-sectional design, which precluded tracking of longitudinal changes in cone density and function in individual patients. Because normal intersubject variability in foveal cone density prevents measurement of absolute photoreceptor loss in individual patients relative to normal, a longitudinal follow-up to the present study would facilitate accurate tracking of degenerative changes measured structurally and functionally. A longitudinal study of AOSLO cone measures was recently published by Talcott et al.,[51] who tracked three patients (two with RP and one with Usher syndrome type 2) treated with sustained-release ciliary neurotrophic factor (CNTF) over 30 to 35 months. Cone spacing increased by 2.9%, and cone density decreased by 9.1% more per year in sham-treated versus CNTF-treated eyes, but no significant changes were observed in VA or visual field sensitivity. These observations indicated preserved visual function, despite significant cone loss in the sham-treated eyes, and a longitudinal follow-up to the present study may produce similar results over a comparable period.

Intrasubject Variability of Psychophysical Measures

Because of the small size and noise of our study's data set, Spearman rank correlation, which is more robust and insensitive to the effects of outliers than regression analysis, was used to evaluate the correlation between cone spacing and visual function. This noise may be partially attributed to intrasubject variability in psychophysical examinations, which is amplified in patients with increased disease severity[8,13,14] because of the inconsistent response of remaining foveal cones to light stimulation. When measuring VA, variations in test procedures (e.g., chart luminance, test distance, and examiner instructions) and indeterminate guessing rates may also increase statistical error.[6] Although the letter-by-letter (ETDRS) scoring protocol used in this study provides higher test-retest reliability than the line assignment method,[6,7] the threshold for significant change in trained, visually normal subjects is still 3.5 to 5 letters.[6,81,82] This variability reinforces the need for more objective measures such as cone structure for assessing retinal health, and future studies should analyze a larger number of eyes and fit the data to regression models to assess whether a continuous relationship exists between foveal cone structure and visual function, taking the variability of clinical measures into account.

Relationship Between Structural Measures and VA

The present study found a significant relationship between foveal cone spacing and VA, which is consistent with previous structure-function correlations using OCT. Multiple groups have reported significant correlations between VA and either IS/OS integrity[28,29] or foveal thickness,[29,31,32] but they did not determine the extent of foveal structural changes before abnormal values were observed psychophysically. Unlike AOSLO data, OCT data have been fit to regression models. In a study of Stargardt disease, Ergun et al.[29] found significant linear relationships between VA and both IS/OS integrity ($R^2 = 0.49$, $P = 0.0001$) and foveal thickness ($R^2 = 0.51$, $P = 0.0001$). Sandberg et al.[32] compared ETDRS acuity and foveal thickness in patients with RP using logarithmic, linear, and second-order polynomial models and found that the second-order polynomial provided the best fits, accounting for a decline in VA at smaller and larger retinal thicknesses because of cone loss and edematous thickening, respectively. Using linear regression, they found a 1.1-letter decrease in ETDRS acuity for every 10-μm decline in foveal thickness, and given their observation that patients with RP on average lose 0.9 letters per year, they calculated the rate of foveal thinning to be 8.2 μm/y. Provided their calculated 38-μm SD for foveal thickness, this roughly predicts a 4-year time course before significant changes are observed structurally with OCT, which is similar to the time it would take to observe significant changes in ETDRS acuity (0.9 letters/y × 4 years = 3.6-letter decrease over 4 years), which is within the threshold range for significant acuity change in visually normal subjects (3.5–5 letters[6,81,82]). As previously mentioned, Talcott et al.[51] observed significant reductions in cone density over the course of 30 to 35 months in the absence of VA changes, suggesting that, although significant structure-function correlations have been observed with both AOSLO and OCT, direct visualization of individual cones as facilitated by AOSLO may provide an earlier measure of structural changes.

Relationship Between Structural Measures and Foveal Sensitivity

The present study found a significant correlation between cone spacing and foveal sensitivity, although cone density thresholds were 52% to 62% below the normal mean before abnormal values were observed in decibel and linear sensitivity. The discrepancy between sensitivity and the structural status of the fovea is likely because of the inadequacy of conventional perimetry stimuli in detecting subtle changes in photoreceptor topography. The SITA standard protocol with a Goldmann III stimulus used in this study is the most common technique for visual field testing, and its 4-mm^2 size translates to a visual angle of 0.12 degree^2 (432 arc min^2) on the retina from a distance of 0.33 meter (m).[83] Given that the diameter of a

normal foveal cone is 0.5 arc min,[63] approximately 2200 foveal cones would sample a Goldmann III stimulus, each corresponding to a single receptive field based on the postreceptoral "private line" hypothesis for foveal cones.[84] This oversampling of numerous receptive fields may lead to an underestimation of subtle visual defects in the tested area because functionally normal cones may conceal regions of dysfunction, providing little insight into the integrity of the local photoreceptor matrix. Although smaller stimulus sizes such as the Goldmann size I (0.0075 degree^2 at 0.33 m) may increase sensitivity to subtle structural defects, their benefits are compromised by the observed increased test-retest variability of smaller stimuli.[83] Because AOSLO images demonstrated up to a 52% to 62% decrease in foveal cones before abnormal changes were observed in sensitivity, these results suggest that structural measures may provide an earlier and more objective assessment of degeneration.

AOSLO-Based Microperimetry for Single-Cell Functional Testing

Adaptive optics scanning laser ophthalmoscopy cone measures assess the integrity of the cone mosaic, but they do not provide information on the functional status of individual cones. Previous studies describe the inconsistent response of remaining foveal cones to light stimulation,[13] and for AOSLO imaging to become a comprehensive and objective measure of disease progression, the structure-function relationship for individual foveal cones needs to be established. Makous et al.[85] used 0.75–arc min AO-corrected stimuli to identify microscotomas in a deuteranopic patient with normal VA and visual field, despite an estimated 30% loss of cone photoreceptors. This result suggests that microperimetry at the resolution of single cones may be necessary for evaluating subtle functional changes in the photoreceptor mosaic indiscernible by standard clinical tests. To enable longitudinal monitoring of individual photoreceptor function, Tuten et al.[86] have developed AOSLO-based microperimetry with real-time eye tracking, facilitating targeted functional testing of individual cones with automatic recovery of previously tested locations. In future studies, AOSLO-based microperimetry may provide insight into the extent of functional changes at the fovea before they are observable by standard clinical measures, providing a more comprehensive understanding of structure-function relationships at the cellular scale.

Structural Measures May Provide More Reliable Predictors of Foveal Degeneration Than Visual Field

For rod-cone degenerations in which peripheral cone loss precedes foveal degeneration, natural history studies predict half-life times of Goldmann V-4e field loss ranging from 5 years ($n = 19$)[18] to 15 years ($n = 90$).[17] Alexander et al.[24] reported that VA loss in patients with RP occurred following the degeneration of parafoveal rods and cones, after which cone IS enlargement was observed to increase foveal cone spacing and decrease the resolution of spatial sampling. Madreperla et al.[87] showed that clinically significant VA loss (<20/40) in patients with RP occurred only after the visual field was constricted to a 15° radius, suggesting that the relationship between VA and visual field radius could help predict the onset of foveal dysfunction in patients. However, this prognosis requires knowledge of the rate of visual field decay, which is highly variable based on differences in visual field loss pattern,[88] critical age,[18,89] disease genotype,[90,91] and environmental and dietary factors.[92,93] Sunga and Sloan[92] reported that rates of visual field loss vary even among family members, with intervals of slow and rapid field loss alternating over the course of an individual's lifetime. Because of these variations, the rate of visual field loss cannot be predicted on an individual basis, precluding the prognosis of foveal degeneration based on peripheral visual field changes. Instead, structural measures such as those provided by AOSLO may be used as an earlier indicator of parafoveal cone changes than visual function, enabling disease monitoring and treatment intervention well before the fovea shows clinical signs of degeneration.

Less Commonly Used Clinical Measures of Function May Be More Sensitive to Structural Changes Than VA or Sensitivity

The aim of the present study was to show that the most commonly reported measures for evaluating foveal function are insensitive indicators of foveal cone structure. However, other psychophysical tests may provide improved sensitivity. Conventional VA tests such as ETDRS charts or Landolt rings use high-contrast figures to assess visual impairment, which may not be as sensitive to foveal degradation as contrast sensitivity tested at various spatial frequencies. Akeo et al.[3] reported significant correlations between Landolt ring VA and Vistech contrast sensitivity at lower spatial frequencies (1.5, 3.0, and 6.0 cycles per degree [cyc/deg]) in patients having RP with greater than 20/50 VA, but at 18.0 cyc/deg a subset of these patients with 20/25 VA had significantly reduced contrast sensitivity (<15 cyc/deg). Using Arden gratings, Lindberg et al.[1] observed similar contrast sensitivity reductions at high frequencies in patients with RP undetected by Snellen acuity, suggesting that abnormalities in patients with preserved VAs may be detectable with contrast gratings at higher spatial frequencies. Despite its advantages, contrast sensitivity is hard to perform routinely (test distance, lighting, and speed of grating presentation need to be precisely controlled,[1] although the development of tablet-based software may make testing conditions more standardized), is more affected by ocular factors such as cataract than conventional VA,[94] and is infrequently used in assessing foveal function. Although the present study did not assess contrast sensitivity, future studies could investigate its correlation with cone structure.

In conclusion, direct, high-resolution images of cone structure such as those provided by AOSLO may provide a more sensitive and more reliable indication of foveal degeneration than VA and foveal sensitivity. These results support the use of AOSLO images as an outcome measure of disease progression and suggest that treatment intervention is best done before measurable vision loss manifests, at which point significant structural changes may have already occurred. Further studies are necessary to determine the exact relationship between cone structure and standard measures of visual function, including large cross-sectional and longitudinal assessments of patients using high-resolution AOSLO images of foveal cones.

Acknowledgments

Supported by an unrestricted grant from Research to Prevent Blindness (JC and JLD); a clinical center grant from the Foundation Fighting Blindness (JLD and AR); an individual investigator grant from the Foundation Fighting Blindness (JC); Grants P30EY001931 and R01EY017607 (JC), EY002162 (JLD), and R01EY014375 (AR) from the National Eye Institute, National Institutes of Health; That Man May See, Inc. (TCP and JLD); The Bernard A. Newcomb Macular Degeneration Fund (JLD); and Hope for Vision (JLD).

Disclosure: **K. Ratnam**, None; **J. Carroll**, Imagine Eyes (S); **T.C. Porco**, None; **J.L. Duncan**, None; **A. Roorda**, P

References

1. Lindberg CR, Fishman GA, Anderson RJ, Vasquez V. Contrast sensitivity in retinitis pigmentosa. *Br J Ophthalmol*. 1981;65:855–858.
2. Wolkstein M, Atkin A, Bodis-Wollner I. Contrast sensitivity in retinal disease. *Ophthalmology*. 1980;87:1140–1149.
3. Akeo K, Hiida Y, Saga M, Inoue R, Oguchi Y. Correlation between contrast sensitivity and visual acuity in retinitis pigmentosa patients. *Ophthalmologica*. 2002;216:185–191.
4. Alexander KR, Hutman LP, Fishman GA. Dark-adapted foveal thresholds and visual acuity in retinitis pigmentosa. *Arch Ophthalmol*. 1986;104:390–394.
5. Birch DG, Sandberg MA, Berson EL. The Stiles-Crawford effect in retinitis pigmentosa. *Invest Ophthalmol Vis Sci*. 1982;22:157–164.
6. Arditi A, Cagenello R. On the statistical reliability of letter-chart visual acuity measurements. *Invest Ophthalmol Vis Sci*. 1993;34:120–129.
7. Vanden Bosch ME, Wall M. Visual acuity scored by the letter-by-letter or probit methods has lower retest variability than the line assignment method. *Eye (Lond)*. 1997;11:411–417.
8. Grover S, Fishman GA, Gilbert LD, Anderson RJ. Reproducibility of visual acuity measurements in patients with retinitis pigmentosa. *Retina*. 1997;17:33–37.
9. Fishman GA, Gilbert LD, Anderson RJ, Marmor MF, Weleber RG, Viana MA. Effect of methazolamide on chronic macular edema in patients with retinitis pigmentosa. *Ophthalmology*. 1994;101:687–693.
10. Seiple W, Clemens CJ, Greenstein VC, Carr RE, Holopigian K. Test-retest reliability of the multifocal electroretinogram and Humphrey visual fields in patients with retinitis pigmentosa. *Doc Ophthalmol*. 2004;109:255–272.
11. Kim LS, McAnany JJ, Alexander KR, Fishman GA. Intersession repeatability of Humphrey perimetry measurements in patients with retinitis pigmentosa. *Invest Ophthalmol Vis Sci*. 2007;48:4720–4724.
12. Ross DF, Fishman GA, Gilbert LD, Anderson RJ. Variability of visual field measurements in normal subjects and patients with retinitis pigmentosa. *Arch Ophthalmol*. 1984;102:1004–1010.
13. Bittner AK, Ibrahim MA, Haythornthwaite JA, Diener-West M, Dagnelie G. Vision test variability in retinitis pigmentosa and psychosocial factors. *Optom Vis Sci*. 2011;88:1496–1506.
14. Kiser AK, Mladenovich D, Eshraghi F, Bourdeau D, Dagnelie G. Reliability and consistency of visual acuity and contrast sensitivity measures in advanced eye disease. *Optom Vis Sci*. 2005;82:946–954.
15. Bailey IL, Bullimore MA, Raasch TW, Taylor HR. Clinical grading and the effects of scaling. *Invest Ophthalmol Vis Sci*. 1991;32:422–432.
16. Massof RW, Dagnelie G, Benzschawel T. First order dynamics of visual field loss in retinitis pigmentosa. *Clin Vis Sci*. 1990;5:1–26.
17. Berson EL, Sandberg MA, Rosner B, Birch DG, Hanson AH. Natural course of retinitis pigmentosa over a three-year interval. *Am J Ophthalmol*. 1985;99:240–251.
18. Iannaccone A, Kritchevsky SB, Ciccarelli ML, et al. Kinetics of visual field loss in Usher syndrome type II. *Invest Ophthalmol Vis Sci*. 2004;45:784–792.
19. Holopigian K, Greenstein V, Seiple W, Carr RE. Rates of change differ among measures of visual function in patients with retinitis pigmentosa. *Ophthalmology*. 1996;103:398–405.
20. Kilbride PE, Fishman M, Fishman GA, Hutman LP. Foveal cone pigment density difference and reflectance in retinitis pigmentosa. *Arch Ophthalmol*. 1986;104:220–224.
21. Elsner AE, Burns SA, Lobes LA Jr. Foveal cone optical density in retinitis pigmentosa. *Appl Opt*. 1987;26:1378–1384.
22. Van Meel GJ, Van Norren D. Foveal densitometry in retinitis pigmentosa. *Invest Ophthalmol Vis Sci*. 1983;24:1123–1130.
23. Geller AM, Sieving PA. Assessment of foveal cone photoreceptors in Stargardt's mascular dystrophy using a small dot detection task. *Vision Res*. 1993;33:1509–1524.
24. Alexander KR, Derlacki DJ, Fishman GA, Szlyk JP. Grating, Vernier, and letter acuity in retinitis pigmentosa. *Invest Ophthalmol Vis Sci*. 1992;33:3400–3406.
25. Flannery JG, Farber DB, Bird AC, Bok D. Degenerative changes in a retina affected with autosomal dominant retinitis pigmentosa. *Invest Ophthalmol Vis Sci*. 1989;30:191–211.
26. Huang D, Swanson EA, Lin CP, et al. Optical coherence tomography. *Science*. 1991;254:1178–1181.
27. Fujimoto JG, Pitris C, Boppart SA, Brezinski ME. Optical coherence tomography: an emerging technology for biomedical imaging and optical biopsy. *Neoplasia*. 2000;2:9–25.
28. Aizawa S, Mitamura Y, Baba T, Hagiwara A, Ogata K, Yamamoto S. Correlation between visual function and photoreceptor inner/outer segment junction in patients with retinitis pigmentosa. *Eye (Lond)*. 2009;23:304–308.
29. Ergun E, Hermann B, Wirtitsch M, et al. Assessment of central visual function in Stargardt's disease/fundus flavimaculatus with ultrahigh-resolution optical coherence tomography. *Invest Ophthalmol Vis Sci*. 2005;46:310–316.
30. Mitamura Y, Mitamura-Aizawa S, Nagasawa T, Katome T, Eguchi H, Naito T. Diagnostic imaging in patients with retinitis pigmentosa. *J Med Invest*. 2012;59:1–11.
31. Witkin AJ, Ko TH, Fujimoto JG, et al. Ultra-high resolution optical coherence tomography assessment of photoreceptors in retinitis pigmentosa and related diseases. *Am J Ophthalmol*. 2006;142:945–952.
32. Sandberg MA, Brockhurst RJ, Gaudio AR, Berson EL. The association between visual acuity and central retinal thickness in retinitis pigmentosa. *Invest Ophthalmol Vis Sci*. 2005;46:3349–3354.
33. Apushkin MA, Fishman GA, Alexander KR, Shahidi M. Retinal thickness and visual thresholds measured in patients with retinitis pigmentosa. *Retina*. 2007;27:349–357.
34. Ratnam K, Västinsalo H, Roorda A, Sankila EM, Duncan JL. Cone structure in patients with Usher syndrome type III and mutations in the *Clarin 1* gene. *JAMA Ophthalmol*. 2013;131:67–74.
35. Yoon MK, Roorda A, Zhang Y, et al. Adaptive optics scanning laser ophthalmoscopy images in a family with the mitochondrial DNA T8993C mutation. *Invest Ophthalmol Vis Sci*. 2009;50:1838–1847.
36. Rangaswamy NV, Patel HM, Locke KG, Hood DC, Birch DG. A comparison of visual field sensitivity to photoreceptor thickness in retinitis pigmentosa. *Invest Ophthalmol Vis Sci*. 2010;51:4213–4219.
37. Liang J, Williams DR, Miller DT. Supernormal vision and high-resolution retinal imaging through adaptive optics. *J Opt Soc Am A Image Sci Vis*. 1997;14:2884–2892.
38. Roorda A, Romero-Borja F, Donnelly W III, Queener H, Hebert T, Campbell M. Adaptive optics scanning laser ophthalmoscopy. *Opt Express*. 2002;10:405–412.
39. Romero-Borja F, Venkateswaran K, Roorda A, Herbert T. Optical slicing of human retinal tissue in vivo with the adaptive optics scanning laser ophthalmoscope. *Appl Opt*. 2005;44:4032–4040.
40. Zhang Y, Poonja S, Roorda A. MEMS-based adaptive optics scanning laser ophthalmoscopy. *Opt Lett*. 2006;31:1268–1270.
41. Duncan JL, Zhang Y, Gandhi J, et al. High-resolution imaging with adaptive optics in patients with inherited retinal degeneration. *Invest Ophthalmol Vis Sci*. 2007;48:3283–3291.
42. Choi SS, Doble N, Hardy JL, et al. In vivo imaging of the photoreceptor mosaic in retinal dystrophies and correlations

with visual function. *Invest Ophthalmol Vis Sci*. 2006;47: 2080–2092.

43. Li KY, Roorda A. Automated identification of cone photoreceptors in adaptive optics retinal images. *J Opt Soc Am A Opt Image Sci Vis*. 2007;24:1358–1363.
44. Rha J, Dubis AM, Wagner-Schuman M, et al. Spectral domain optical coherence tomography and adaptive optics: imaging photoreceptor layer morphology to interpret preclinical phenotypes. *Adv Exp Med Biol*. 2010;664:309–316.
45. Roorda A, Zhang Y, Duncan JL. High-resolution in vivo imaging of the RPE mosaic in eyes with retinal disease. *Invest Ophthalmol Vis Sci*. 2007;48:2297–2303.
46. Wolfing JI, Chung M, Carroll J, Roorda A, Williams DR. High-resolution retinal imaging of cone-rod dystrophy. *Ophthalmology*. 2006;113:1019.e1. Available at: http://www.aaojournal.org/article/S0161-6420(06)00154-0/abstract. Accessed August 1, 2013.
47. Merino D, Duncan JL, Tiruveedhula P, Roorda A. Observation of cone and rod photoreceptors in normal subjects and patients using a new generation adaptive optics scanning laser ophthalmoscope. *Biomed Opt Express*. 2011;2:2189–2201.
48. Duncan JL, Talcott KE, Ratnam K, et al. Cone structure in retinal degeneration associated with mutations in the *peripherin/RDS* gene. *Invest Ophthalmol Vis Sci*. 2011;52:1557–1566.
49. Chen Y, Ratnam K, Sundquist SM, et al. Cone photoreceptor abnormalities correlate with vision loss in patients with Stargardt disease. *Invest Ophthalmol Vis Sci*. 2011;52:3281–3292.
50. Duncan JL, Ratnam K, Birch DG, et al. Abnormal cone structure in foveal schisis cavities in X-linked retinoschisis from mutations in exon 6 of the *RS1* gene. *Invest Ophthalmol Vis Sci*. 2011;52:9614–9623.
51. Talcott KE, Ratnam K, Sundquist SM, et al. Longitudinal study of cone photoreceptors during retinal degeneration and in response to ciliary neurotrophic factor treatment. *Invest Ophthalmol Vis Sci*. 2011;52:2219–2226.
52. Duncan JL, Roorda A, Navani M, et al. Identification of a novel mutation in the *CDHR1* gene in a family with recessive retinal degeneration. *Arch Ophthalmol*. 2012;130:1301–1308.
53. Ahnelt PK. The photoreceptor mosaic. *Eye (Lond)*. 1998;12: 531–540.
54. Putnam NM, Hammer DX, Zhang Y, Merino D, Roorda A. Modeling the foveal cone mosaic imaged with adaptive optics scanning laser ophthalmoscopy. *Opt Express*. 2010;18:24902–24916.
55. Dubra A, Sulai Y. Reflective afocal broadband adaptive optics scanning ophthalmoscope. *Biomed Opt Express*. 2011;2: 1757–1768.
56. Li KY, Mishra S, Tiruveedhula P, Roorda A. Comparison of control algorithms for a MEMS-based adaptive optics scanning laser ophthalmoscope. *Proc Am Control Conf*. 2009;2009: 3848–3853.
57. Dubra A, Sulai Y, Norris JL, et al. Noninvasive imaging of the human rod photoreceptor mosaic using a confocal adaptive optics scanning ophthalmoscope. *Biomed Opt Express*. 2011; 2:1864–1876.
58. Li K, Tiruveedhula P, Roorda A. Intersubject variability of foveal cone photoreceptor density in relation to eye length. *Invest Ophthalmol Vis Sci*. 2010;51:6858–6867.
59. Rossi EA, Roorda A. The relationship between visual resolution and cone spacing in the human fovea. *Nat Neurosci*. 2010;13:156–157.
60. Carroll J, Dubra A, Gardner JC, et al. The effect of cone opsin mutations on retinal structure and the integrity of the photoreceptor mosaic. *Invest Ophthalmol Vis Sci*. 2012;53: 8006–8015.
61. Early Treatment Diabetic Retinopathy Study Research Group. Photocoagulation for diabetic macular edema: Early Treatment Diabetic Retinopathy Study report number 1. *Arch Ophthalmol*. 1985;103:1796–1806.
62. Poonja S, Patel S, Henry L, Roorda A. Dynamic visual stimulus presentation in an adaptive optics scanning laser ophthalmoscope. *J Refract Surg*. 2005;21:S575–S580.
63. Putnam NM, Hofer HJ, Doble N, Chen L, Carroll J, Williams DR. The locus of fixation and the foveal cone mosaic. *J Vis*. 2005;5: 632–639.
64. Geller AM, Sieving PA, Green DG. Effect on grating identification of sampling with degenerate arrays. *J Opt Am A*. 1992; 9:472–477.
65. Chui TY, Song H, Burns SA. Adaptive-optics imaging of human cone photoreceptor distribution. *J Opt Soc Am A Opt Image Sci Vis*. 2008;25:3021–3029.
66. Curcio CA, Sloan KR, Kalina RE, Hendrickson AE. Human photoreceptor topography. *J Comp Neurol*. 1990;292:497–523.
67. Chui TY, Song H, Burns SA. Individual variations in human cone photoreceptor packing density: variations with refractive error. *Invest Ophthalmol Vis Sci*. 2008;49:4679–4687.
68. Song H, Chui TY, Zhong Z, Elsner AE, Burns SA. Variation of cone photoreceptor packing density with retinal eccentricity and age. *Invest Ophthalmol Vis Sci*. 2011;52:7376–7384.
69. Ferris FL, Kassoff A, Bresnick GH, Bailey J. New visual acuity charts for clinical research. *Am J Ophthalmol*. 1982;94:91–96.
70. Davison AC, Hinkley DV. *Bootstrap Methods and Their Application*. Cambridge, UK: Cambridge University Press; 1997. Cambridge Series in Statistical and Probabilistic Mathematics.
71. Barlow HB. Eye movements during fixation. *J Physiol*. 1952; 116:290–306.
72. Ditchburn RW. *Eye-Movements and Visual Perception*. Oxford, UK: Clarendon Press; 1973.
73. Steinman RM, Haddad GM, Skavenski AA, Wyman D. Miniature eye movement. *Science*. 1973;181:810–819.
74. Panda-Jonas S, Jonas JB, Jakobczyk-Zmija M. Retinal photoreceptor density decreases with age. *Ophthalmology*. 1995;102: 1853–1859.
75. Bennett AG, Rudnicka AR, Edgar DF. Improvements on Littman's method of determining the size of retinal features by fundus photography. *Graefes Arch Clin Exp Ophthalmol*. 1994;232:361–367.
76. Rossi EA, Weiser P, Tarrant J, Roorda A. Visual performance in emmetropia and low myopia after correction of high-order aberrations. *J Vis*. 2007;7:14. Available at: http://www.journalofvision.org/content/7/8/14.long. Accessed August 1, 2013.
77. Marcos S, Navarro R. Determination of the foveal cone spacing by ocular speckle interferometry: limiting factors and acuity predictions. *J Opt Soc Am A Opt Image Sci Vis*. 1997;14:731–740.
78. Weymouth FW, Hines DC, Acres LH, Raaf JE, Wheeler MC. Visual acuity within the area centralis and its relation to eye movements and fixation. *Am J Ophthalmol*. 1928;11:947–960.
79. Eagle RC Jr, Lucier AC, Bernardino VB Jr, Yanoff M. Retinal pigment epithelial abnormalities in fundus flavimaculatus: a light and electron microscopic study. *Ophthalmology*. 1980; 87:1189–1200.
80. Seiple W, Holopigian K, Szlyk JP, Greenstein VC. The effects of random element loss on letter identification: implications for visual acuity loss in patients with retinitis pigmentosa. *Vision Res*. 1995;35:2057–2066.
81. Elliott DB, Sheridan M. The use of accurate visual acuity measurements in clinical anti-cataract formulation trials. *Ophthalmic Physiol Opt*. 1988;8:397–401.

Investigative Ophthalmology & Visual Science

82. Bailey IL, Lovie JE. New design principles for visual acuity letter charts. *Am J Optom Physiol Opt*. 1976;53:740–745.
83. Vislisel JM, Doyle CK, Johnson CA, Wall M. Variability of rarebit and standard perimetry sizes I and III in normals. *Optom Vis Sci*. 2011;88:635–639.
84. Dacey DM. The mosaic of midget ganglion cells in the human retina. *J Neurosci*. 1993;13:5334–5355.
85. Makous W, Carroll J, Wolfing JI, Lin J, Christie N, Williams DR. Retinal microscotomas revealed with adaptive-optics microflashes. *Invest Ophthalmol Vis Sci*. 2006;47:4160–4167.
86. Tuten WS, Tiruveedhula P, Roorda A. Adaptive optics scanning laser ophthalmoscope–based microperimetry. *Optom Vis Sci*. 2012;89:563–574.
87. Madreperla SA, Palmer RW, Massof RW, Finkelstein D. Visual acuity loss in retinitis pigmentosa: relationship to visual field loss. *Arch Ophthalmol*. 1990;108:358–361.
88. Grover S, Fishman GA, Anderson RJ, Alexander KR, Derlacki DJ. Rate of visual field loss in retinitis pigmentosa. *Ophthalmology*. 1997;104:460–465.
89. Fishman GA, Bozbeyoglu S, Massof RW, Kimberling W. Natural course of visual field loss in patients with type 2 Usher syndrome. *Retina*. 2007;27:601–608.
90. Sadeghi AM, Eriksson K, Kimberling WJ, Sjostrom A, Moller C. Longterm visual prognosis in Usher syndrome types 1 and 2. *Acta Ophthalmol Scand*. 2006;84:537–544.
91. Sandberg MA, Rosner B, Weigel-DiFranco C, Dryja TP, Berson EL. Disease course of patients with X-linked retinitis pigmentosa due to *RPGR* gene mutations. *Invest Ophthalmol Vis Sci*. 2007;48:1298–1304.
92. Sunga RN, Sloan LL. Pigmentary degeneration of the retina: early diagnosis and natural history. *Invest Ophthalmol Vis Sci*. 1967;6:309–325.
93. Hartong DT, Berson EL, Dryja TP. Retinitis pigmentosa. *Lancet*. 2006;18:1795–1809.
94. Elliott DB. Evaluating visual function in cataract. *Optom Vis Sci*. 1993;70:896–902.
95. Syed R, Sundquist SM, Ratnam K, et al. High resolution images of retinal structure in patients with choroideremia. *Invest Ophthalmol Vis Sci*. 2013;54:950–961.

Investigative Ophthalmology & Visual Science